Evaluation of Residual Axial Load Capacity of RC Columns after Shear Failure

Y. Yang

Department of Architecture, The University of Tokyo, Tokyo, Japan

K. Matsukawa, H. Choi & Y. Nakano

Institute of Industrial Science, The University of Tokyo, Tokyo, Japan

ABSTRACT: This paper introduces an arch resistance model to evaluate the residual axial load carrying capacity of a Reinforced Concrete (RC) column, which has suffered severe shear failure due to a large earthquake. The proposed arch resistance model, based on the theory of structural mechanics, can give a better understanding of the loss of axial load carrying capacity of a RC column. The evaluation formula of the residual axial load carrying capacity, which consists of longitudinal reinforcement and confined concrete contributions, is also derived based on the proposed model. In addition, the database of loading tests carried out by other researchers is also compiled to verify the formula. The estimation results by the proposed formula show a good agreement with test results.

1 INTRODUCTION

From the post-earthquake reconnaissance survey, it is observed that reinforced concrete (RC) short columns and RC columns with poor transverse reinforcement are vulnerable to shear failure. For severely shear-damaged RC columns without adjacent load redistribution members around them, the deterioration of the axial load carrying capacity of these damaged columns can lead to a global or partial building collapse (Fig. 1). For existing columns vulnerable to shear failure as mentioned above, it is therefore necessary to evaluate the residual axial load carrying capacity and to give advice for seismic resistance evaluation or seismic retrofit.

Until now, several evaluation models have been proposed by other researchers to account for the loss of axial load carrying capacity for such RC columns prone to shear failure. Uchida and Uezono (2003) have presented an evaluation model based on the principle of virtual work to predict the residual axial load carrying capacity. Elwood and Moehle (2005) have developed a shear-friction model to predict the drift angle at which axial collapse occurs. Takaine and Yoshimura (2007) have also proposed an evaluation model to estimate the axial load carrying capacity after shear failure, based on the concept of reduced failure surface and regression analysis of several tests results. However, for RC columns failed in shear (Fig. 2), when the cover concrete is totally removed and the confined core concrete is completely crushed under earthquake motions, it is not easy to obtain an intuitive understanding regarding the loss of axial load carrying capacity through these models.

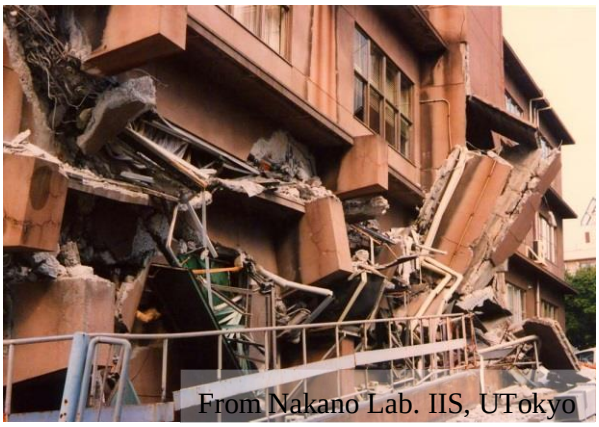

Fig. 1. Axial collapse (1995 Kobe Earthquake)

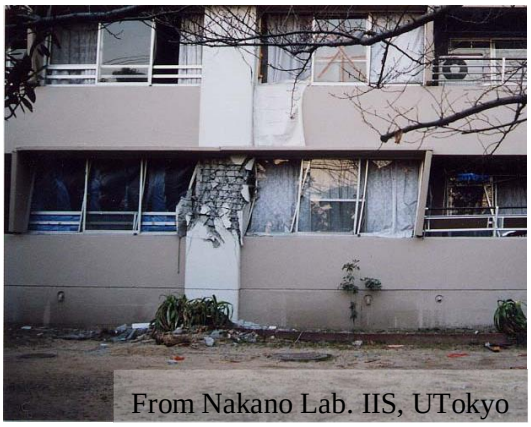

Fig. 2. Shear failure (1995 Kobe Earthquake)

Hence, in this paper, an arch resistance model is presented for shear damaged RC columns with crushed core concrete, which can give a better understanding of the loss of axial load carrying capacity. This model is deduced based on the theory of structural mechanics and observations made on RC columns heavily damaged in shear. The derivation of the evaluation formula is also presented in this paper. In addition, the database of several loading tests carried out by other researchers is also compiled to verify the evaluation formula.

2 DEVELOPMENT OF THE ARCH RESISTANCE MODEL

2.1 Definition of limit state of axial collapse

In this section, for a RC column with crushed core concrete, as shown in Fig. 3, the limit state of axial collapse is defined by analysing the change in internal force (Q, N and M), at both end sections of shear failed portion with horizontal displacement. It can be considered that the rotation of the shear failed portion ends is restrained by the upper and lower floor slabs or non-structural walls and the internal moments at the end sections are equal to each other. Thus, for the shear failed portion, the equilibrium equation of moment can be written as Eq. (1) and the internal moment at the end sections can be expressed as Eq. (2). When the axial force is a constant, the change of internal moment with horizontal displacement can be shown as Fig. 4. The bending moment ($0.5N\delta$) contributed by axial force linearly behaves with horizontal displacement. However, the bending moment ($0.5QL$) provided by shear force is non-linear because the yielding occurs at both ends and it decreases along with increase in horizontal displacement. When the shear force degrades to zero with increase in horizontal displacement, the total bending moment acting on the end sections is equal to the maximum moment capacity of column section (as shown by (A) in the figure). If the horizontal displacement increases further, the equilibrium between internal forces and moments will be lost and the axial collapse will take place. It can be conclude that the state of shear force equal to zero is the limit state of equilibration at which the horizontal displacement reaches a maximum. In this paper, for a RC column under a constant axial force with increase in horizontal displacement, the state of shear force equal to zero is defined as the limit state of axial collapse.

At the defined limit state of axial collapse, the residual axial load carrying capacity can be considered equal to the constant axial force. In this paper, this characteristic will be used to develop the evaluation model of residual axial load carrying capacity.

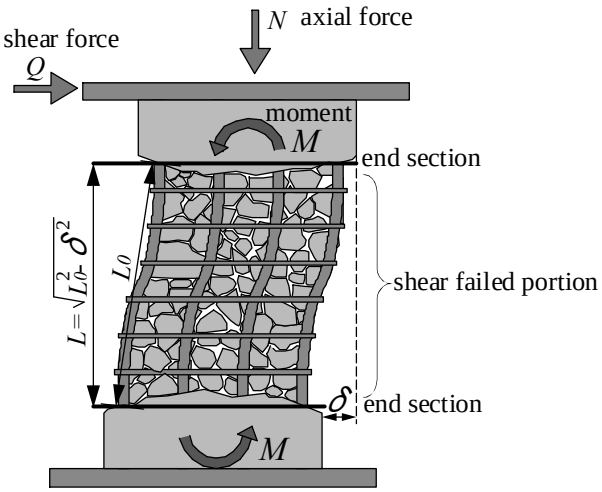

Fig. 3. Free body diagram of shear failed portion with crushed core concrete

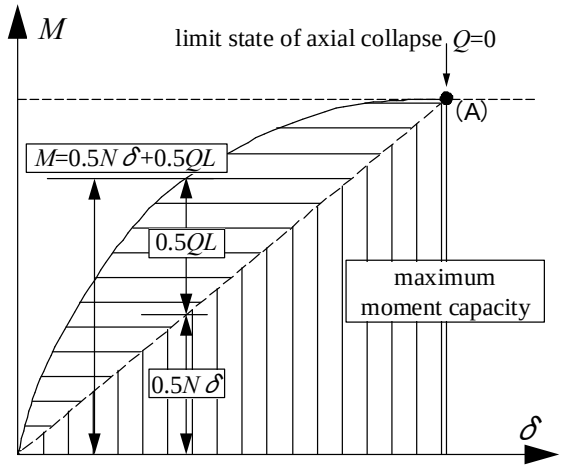

Fig. 4. Relationship between internal moment and horizontal displacement at the end sections

$$2M = N\delta + QL \tag{1}$$

$$M = 0.5N\delta + 0.5QL \tag{2}$$

where N =the axial force; Q =the shear force; M =the bending moment of the end sections; L_0 = the length of shear failure portion in axial direction; and L = the length of shear failure portion in vertical direction.

2.2 **Arch resistance model**

For a shear failed RC column at the limit state of axial collapse, as shown in Fig. 3, when the cover concrete is totally spalled off and the confined core concrete is completely crushed due to an earthquake, an arch resistance model (see Fig. 5) can be developed under the following assumptions.

1. The bond strength between the reinforcing bars and concrete can be neglected and no transmission of forces is expected between longitudinal reinforcement and crushed core concrete.

2. No rotation is expected at the ends of the shear failed portion.

3. Every longitudinal steel bar has the same internal forces and moments at end sections.

4. The buckling of longitudinal reinforcement does not happen prior to the axial collapse.

5. Confined core concrete cannot resist any bending moment as the core concrete is crushed completely.

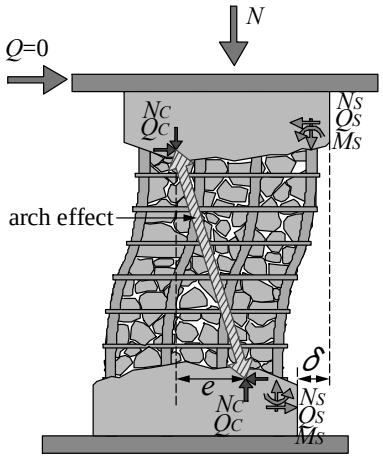

(The symbols of internal forces at longitudinal bar end sections are only indicated for one of bars.)

Fig. 5. Arch resistance model

According to the definition of the limit state of axial collapse, the sum of shear forces of longitudinal steel bars and confined core concrete equals to zero (Eq. (3)) and the equilibrium equation of moment is shown in Eq. (4). It reveals that if the axial force of confined core concrete (N_c), the eccentricity (e) of axial forces carried by confined core concrete, and the relationship between axial force (N_S) and moment (M_S) of longitudinal steel bar are given, the axial force (N_S) of longitudinal steel bar can be obtained.

It should be noted that in this model the axial forces acting with an eccentricity e at the end sections of confined core concrete part can develop a force couple, which resists in the moment induced by the P-Δ effect of longitudinal steel bars (Eq. (4)). The resistance of the force couple ($N_c e$) acting on the crushed core concrete can be considered as the interaction between crushed core concrete and longitudinal steel bars and it is called ‘arch effect’ in this research.

$$nQ_S + Q_C = 0 \tag{3}$$

$$nN_S\delta = 2nM_S + N_C e \tag{4}$$

where N=the residual axial load carrying capacity; N_S=the axial force carried by each longitudinal steel bar; Q_S=the shear force carried by each longitudinal steel bar; M_S=the bending moment carried by each longitudinal steel bar; N_C=the axial force carried by confined core concrete part; Q_C =the shear force carried by confined core concrete part; e=the eccentricity of axial forces carried by confined core concrete; δ=the horizontal displacement; n=the number of longitudinal steel bars.

2.3 **Axial force carried by confined core concrete part N_C**

The formula of axial force carried by confined core concrete is deduced based on the equilibrium of forces shown in the free body diagram (Fig. 6) and the following assumptions.

1. At the inclined and horizontal cutting plane, the relationship of forces parallel and perpendicular to the cutting plane is subject to the Coulombôs law of friction.

2. The plastic strength of all transverse reinforcement of the shear failed portion can be achieved fully under the tensile action induced by the crushed confined core concrete.

The equilibrium equations of horizontal and vertical direction of forces shown in the free body diagram (Fig. 6) can be given as Eq. (5) and Eq. (6). The axial force of confined core concrete can be given as Eq. (7) by solving Eq. (5) and Eq. (6). Also, the equilibrium (Eq. (8) of moment at point O shown in Fig. 6,) can be developed to obtain the eccentricity *e* of the axial load acting on the end sections of confined core concrete, as shown in Eq. (9).

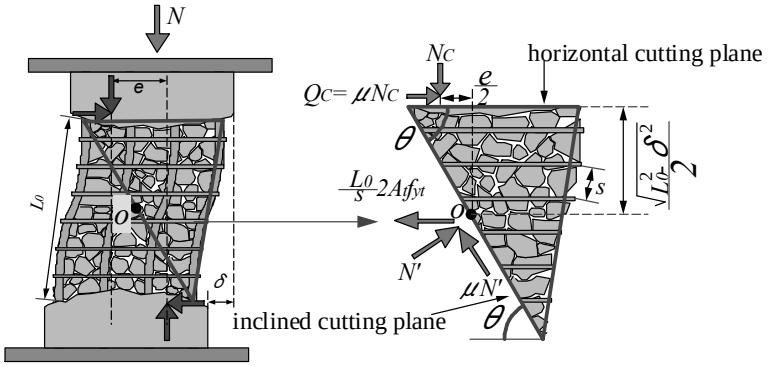

Fig. 6. Free body diagram of confined core concrete

$$\mu N_C + N' \sin\theta = \mu N' \cos\theta + \frac{L_0}{s} 2A_t f_{yt} \tag{5}$$

$$N_C = \mu N' \sin\theta + N' \cos\theta \tag{6}$$

$$N_C = \frac{L_0}{s} 2A_t f_{yt} \frac{\mu \sin\theta + \cos\theta}{\mu^2 \sin\theta + \sin\theta} \tag{7}$$

$$N_C(\frac{e}{2}) = \mu N_C(\frac{\sqrt{L_0^2 - \delta^2}}{2}) \tag{8}$$

$$e = \mu\sqrt{L_0^2 - \delta^2} \tag{9}$$

where θ= the inclination of cutting plane; s= the spacing of transverse reinforcement; A_t= the section area of transverse reinforcement; f_{yt}= the yield strength of transverse reinforcement; N= the compressive force perpendicular to the inclined cutting plan; μ= the friction factor.

2.4 **Axial force carried by longitudinal reinforcement bars N_S**

As mentioned above, except for the axial force (N_C) carried by confined core concrete and its eccentricity (e) obtained in the above section, the relationship between axial force (N_S) and moment (M_S) of longitudinal steel bar is also required to obtain the axial force carried by longitudinal reinforcing bars. Thus, in order to derive the relationship between axial force and moment of longitudinal steel bar, as shown in Fig.7, it is assumed that at the limit state of axial collapse, the end sections of longitudinal bars reach a fully plastic condition. By stress integration method, axial force and bending moment can be obtained.

For easier development of the relationship between axial force and moment for longitudinal bars, the ideal circular cross section is applied neglecting the effect of steel ribs. The elasto-plastic mechanical property is adopted neglecting strain hardening. The bending moment and axial force acting on the end sections of longitudinal bars can be expressed as Eqs. (10) and (11). From them, the initial relationship between axial force and moment of longitudinal bars can be obtained, as shown in Eq. (12). The distance *h* from centroid of area A to the centreline in Eq. (12) and Fig. 17 can be determined by Eq. (13). The axial force can also be obtained by stress integration over compressive part of end section, as

shown in Eq. (14). By eliminating the parameter *x* and *h,* and by combining the three equations (Eqs. (12), (13) and (14)), the final relationship between axial force and moment of longitudinal bars can be shown as Eq. (15). By solving the equations (Eqs. (6), (9) and (15)), the axial force of longitudinal bars can be determined. However, it is difficult to obtain an explicit function for axial force of longitudinal bars in terms of horizontal displacement and it is too complex for practical applications. So, for the actual practice of seismic resistance evaluation or seismic retrofit, the interaction relationship between axial force and moment needs to be simplified to obtain an explicit function for axial force of longitudinal bars.

Thus, by using the elliptic function (Fig.8, Eq. (16)) to approximate the interaction relationship between axial force and moment (Eq. (15)), an explicit function for axial force of longitudinal bars can be obtained (Eq. (17)). As shown in Fig.8, compared with linear approximation (introduced by EIwood and Moehle, 2005), the method proposed in this paper has a relatively high accuracy, although the formula itself is complex.

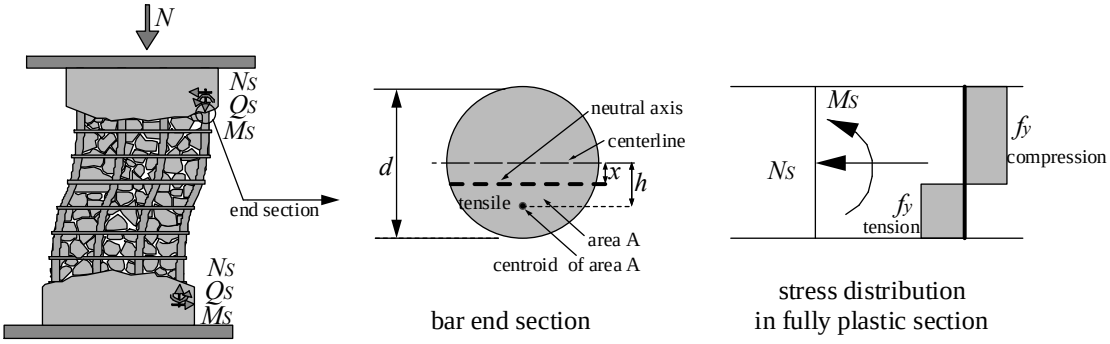

Fig. 7. Ideal plastic section at the ends of longitudinal bars for the shear failed portion

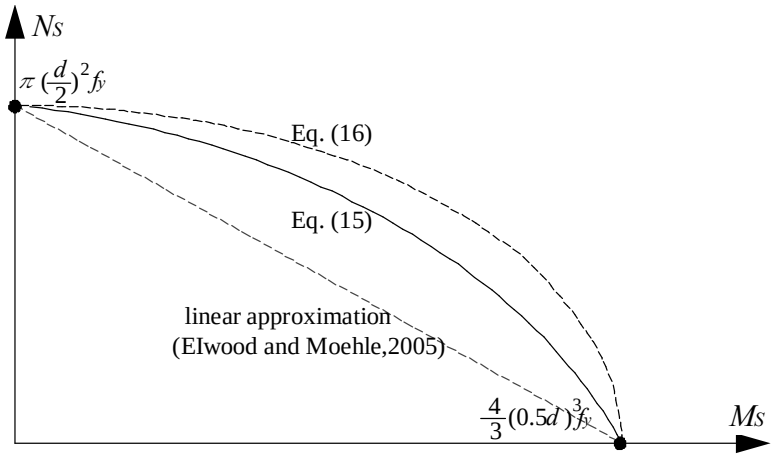

Fig. 8. Axial force and moment interaction relationship

$$M_S = 2Af_y h \tag{10}$$

$$N_S = (\pi\left(\frac{d}{2}\right)^2 - 2A) f_y \tag{11}$$

$$M_S = (\pi\left(\frac{d}{2}\right)^2 f_y - N_S)h \tag{12}$$

$$h = \frac{\frac{2}{3}\left[\left(\frac{d}{2}\right)^2 - x^2\right]^{\frac{3}{2}}}{\frac{1}{2}(\pi\left(\frac{d}{2}\right)^2 - \frac{N_S}{f_y})} \tag{13}$$

$$N_S = 2(2\int_0^{\arcsin(\frac{x}{\frac{d}{2}})} \frac{1}{2}(\frac{d}{2})^2 d\theta + x\sqrt{(\frac{d}{2})^2 - x^2})f_y \tag{14}$$

$$\left(\frac{d}{2}\right)^2 \times \arcsin\left(\frac{\sqrt{\left(\frac{d}{2}\right)^2 - (\frac{3M_S}{4f_y})^{\frac{2}{3}}}}{\frac{d}{2}}\right) + \sqrt{\left(\frac{d}{2}\right)^2 - (\frac{3M_S}{4f_y})^{\frac{2}{3}}}(\frac{3M_S}{4f_y})^{\frac{1}{3}} = \frac{N_S}{2f_y} \tag{15}$$

$$\frac{N_S^2}{(\pi\left(\frac{d}{2}\right)^2 f_y)^2} + \frac{M_S^2}{(\frac{4}{3}(\frac{d}{2})^3 f_y)^2} = 1 \tag{16}$$

$$N_S = \frac{\frac{N_C e\delta}{2n(\frac{4}{3}(\frac{d}{2})^3 f_y)^2} + \sqrt{\left[\frac{N_C e\delta}{2n(\frac{4}{3}(\frac{d}{2})^3 f_y)^2}\right]^2 - 4\left[\frac{1}{(\pi\left(\frac{d}{2}\right)^2 f_y)^2} + \frac{\delta^2}{(\frac{8}{3}(\frac{d}{2})^3 f_y)^2}\right]\cdot\left[\frac{N_C^2 e^2}{(\frac{8}{3}(\frac{d}{2})^3 f_y n)^2} - 1\right]}}{2\left[\frac{1}{(\pi\left(\frac{d}{2}\right)^2 f_y)^2} + \frac{\delta^2}{(\frac{8}{3}(\frac{d}{2})^3 f_y)^2}\right]} \tag{17}$$

where d=the diameter of longitudinal bar; f_y=the yield strength of longitudinal bar. A= the area of compressive part of end section. h= the distance from centroid of area A to the centreline. x=the distance between neutral axis and centreline.

2.5 **Residual axial load capacity of RC columns after shear failure**

Therefore, the residual axial load carrying capacity can be evaluated as Eq. (18), consisting of longitudinal reinforcing bars and confined core concrete contributions.

$$N = nN_S + N_C \tag{18}$$

3 APPLICATION OF THE ARCH RESISTANCE MODEL

To verify the accuracy of the formula of residual axial load carrying capacity proposed above, a database of test results from several shear failed RC column specimens are compiled (Table 1). In the verification, the following assumptions are made.

1. The critical shear crack angle (the angle between the crack surface and longitudinal direction of column when the column fails in shear) for shear-critical column can be taken as 60° (Kato D., Li Z., Nakamura Y., and Honda Y., 2007). To estimate the concrete contribution to residual axial load carrying capacity (Eq. (7)), the length L_0 of shear failed portion is required and it can be determined by the critical shear crack angle and the depth of column section.

2. The friction factor μ is adopted as 0.6 (Architectural Institute of Japan, 2002) neglecting the interlocking effect of crushed concrete. Although it is reported (Elwood and Moehle, 2005) that the friction factor (as shown in Fig. 6) is a function of the drift angle when axial failure occurs, it is taken as a constant value of 0.6 to simplify the formula in this paper.

The comparison between the calculated and measured results of the residual axial load carrying capacity is shown in Fig. 9(a). As can be found in the figure, the calculated results have a good agreement with the measured results except for specimens with transverse reinforcement ratio more than 0.51% (PG1.7 and PG3.0). For the specimens PG1.7 and PG3.0, the proposed formula of residual axial load carrying capacity leads to overestimated results. It is possibly because the yield capacity is not achieved fully in the transverse reinforcement of shear failure portion at the limit state of axial collapse and this is not consistent with the assumption mentioned above. The valid range of transverse reinforcement ratio for this assumption should be further discussed in the future.

Table 1. Database of shear failed columns

Specimen	D (mm)	b (mm)	h (mm)	d (mm)	n	f_y (MPa)	ρ (%)	d_t (mm)	s (mm)	f_{yt} (MPa)	ρ_t (%)	N_R (kN)	δ (mm)
Ryu Y., Nakamura T., and Yoshimura M., 2001													
N27C	300	300	900	15.9	12	380	2.65	6.35	100	375	0.21	644	27
N18M	300	300	900	15.9	12	380	2.65	6.35	100	375	0.21	429	83
N27M	300	300	900	15.9	12	380	2.65	6.35	100	375	0.21	644	42
Ishigami S., Owa Seira., Nakamura Takaya., and Yoshimura M., 2002													
2C	300	300	600	15.9	12	396	2.65	6.35	100	392	0.21	431	47
3C	300	300	600	15.9	12	396	2.65	6.35	100	392	0.21	657	32
2M	300	300	600	15.9	12	396	2.65	6.35	100	392	0.21	431	40
3M	300	300	600	15.9	12	396	2.65	6.35	100	392	0.21	657	22
2M13	300	300	600	12.7	12	350	1.69	6.35	100	392	0.21	431	22
Yoshimura M., Takaine Y., and Nakamura T., 2004													
NO.3	300	300	1200	15.9	12	402	2.65	6.35	200	392	0.11	553	23
NO.4	300	300	1200	15.9	12	402	2.65	6.35	100	392	0.21	829	30
NO.5	300	300	1200	15.9	12	402	2.65	6.35	100	392	0.21	967	24
Yamanaka N., and Yoshimura M., 2000													
S1	400	400	900	22.2	16	547	3.87	9.53	180	355	0.20	803	88
S2	400	400	900	22.2	16	547	3.87	9.53	180	355	0.20	803	71
Kato D., Li Z., Nakamura Y., and Honda Y. 2006													
D13W-1	180	180	360	12.7	4	335	1.56	6.35	70	335	0.51	300	12
Nakamura T., Muto S., Ito S., and Yoshimura M., 2011													
PG1.7	450	450	900	19.1	12	390	1.70	9.53	60	390	0.53	911	69
PG3.0	450	450	900	25.4	12	390	3.00	9.53	60	390	0.53	911	127

Note: D=the column section depth; b=the column section width; h=the column interior net height; d=the diameter of longitudinal bar; n= the number of longitudinal bar; f_y=the yield strength of longitudinal bar; ρ=the longitudinal reinforcement ratio; d_t=the diameter of transverse reinforcement; s=the spacing of transverse reinforcement; f_{yt} =the yield strength of transverse reinforcement; ρ_t=the transverse reinforcement ratio; N_R=the residual axial load carrying capacity (at the defined limit state equal to constant axial force); δ=the horizontal displacement (convert from the drift angle at which the shear force equal to zero)

In addition to the application of the arch resistance model proposed in this paper, the shear-friction model introduced by EIwood and Moehle (2005) is also examined using same database shown in Table 1. In the application of the shear-friction model, the depth of column core d_c(centreline to centreline of transverse reinforcement) is taken as 0.8 times of the depth of column; The critical shear crack angle is adopted as 65° (EIwood and Moehle, 2005); The friction factor μ is adopted as a constant value of 0.6 to simplify the application process of the model, although it is reported (Elwood and Moehle, 2005) that the friction factor is a function of the drift angle when axial failure occurs.

The result of application (Fig. 9(b)) shows that the shear-friction model gives underestimations of the residual axial load capacity for most of the specimens. This is primarily because that the interaction between crushed core concrete and longitudinal steel bars is not considered in the shear-friction model. As described in section 2.2, this interaction is taken into account in the evaluation model proposed in this research, which can give a better estimation of the residual axial load capacity.

4 CONCLUSIONS

Based on the theory of structural mechanics and the observation of RC columns severely damaged in shear, the arch resistance model to predict residual axial load carrying capacity is proposed and its accuracy is discussed by comparing data provided by the precious tests. For most of the specimens included in the compiled database, the estimated residual axial capacity has a good agreement with the

measured results. However, it overestimated the results for specimens with high lateral reinforcement ratios (PG1.7 and PG3.0) and the stress distribution assumption for transverse reinforcement is needed to improve the model for RC columns with a high transverse reinforcement ratio.

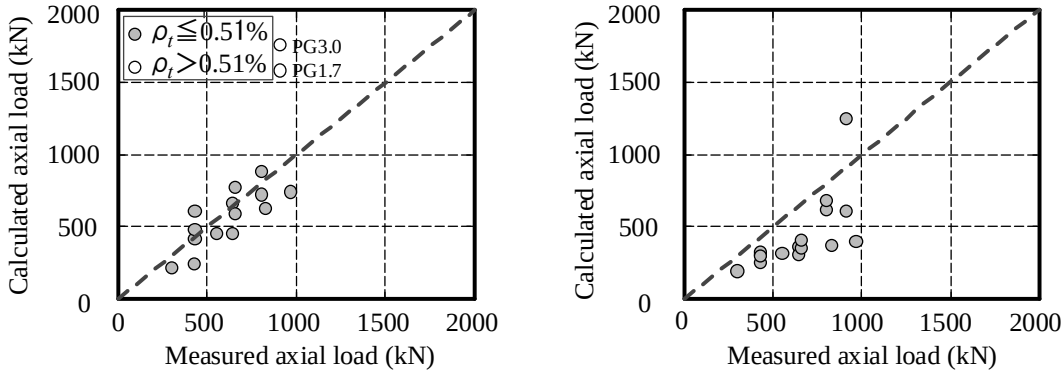

(a) Arch resistance model (b) Shear-friction model

Fig. 9. Comparison of calculated-to-measured residual axial load carrying capacity

5 ACKNOWLEGMENT

The study was supported by JAPAN SOCIETY FOR THE PROMOTION OF SCIENCE under Grant No. 24246093 (Principal investigator: Y. Nakano) and LIXIL JS Foundation under Grant No.13-25 (Principal investigator: K. Matsukawa). This support is greatly acknowledged. All opinions expressed in this paper are solely those of the authors and do not necessarily represent the views of the sponsors.

REFERENCES:

Architectural Institute of Japan. 2002. AIJ Guidelines for the Design of Structural Precast Concrete Emulating Cast-in-place Reinforced Concrete. *Tokyo: Architectural Institute of Japan*. (in Japanese)

EIwood K.J., Moehle J.P. 2005. Axial capacity model for shear-damaged columns. *ACI Structural Journal*. 102. 578-587.

Ishigami S., Owa Seira., Nakamura Takaya., and Yoshimura M. 2002. Axial load carrying capacity of shear-failing RC short columns: Part1 Outline of tests, axial deformation-lateral deformation relations and collapse behaviro. *Summaries of Technical Papers of Annual Meeting Architectural Institute of Japan*. 391-392. (in Japanese)

Kato D., Li Z., Nakamura Y., and Honda Y. 2006. Tests on axial load capacity of shear failure R/C columns considering reinforcing details: relationship between axial loading test and lateral loading test. *Journal of Structural and Construction Engineering*. 610. 153-159. (in Japanese)

Kato D., Li Z., Nakamura Y., and Honda Y. 2007. Experimental study on residual axial load capacity of R/C columns. *Journal of Structural and Construction Engineering*. 619. 127-132. (in Japanese)

Nakamura T., Muto S., Ito S., and Yoshimura M. 2011. Effect of longitudinal reinforcement ratio on seismic performance of RC columns with shear mode: collapse test of RC short columns with large hoop ratio. *Summaries of Technical Papers of Annual Meeting Architectural Institute of Japan*. 161-162. (in Japanese)

Ryu Y., Nakamura T., and Yoshimura M. 2001. Axial load carrying capacity of RC columns subjected to seismic actions. *Proceedings of the Japan Concrete Institute*. 23 (3). 217-222. (in Japanese)

Takaine Y., and Yoshimura M. 2007. Damage evaluation of R/C shear columns based on concept of failure surface contraction. *Journal of Structural and Construction Engineering*. 618. 191-197. (in Japanese)

Uchida Y., and Uezono Y. 2003. Judging collapse of SRC and RC columns failed by shear. *Journal of Structural and Construction Engineering*. 566. 177-184. (in Japanese)

Yamanaka N., and Yoshimura M. 2000. Collapse of Flexure-shear and shear failing RC columns subjected to low axial load. *Proceedings of the Japan Concrete Institute*. 22 (3). 325-330. (in Japanese)

Yoshimura M., Takaine Y., and Nakamura T. 2004. Axial Collapse of Reinforced Concrete Columns. *The 13th World Conference Earthquake Engineering*, Paper No.1699.